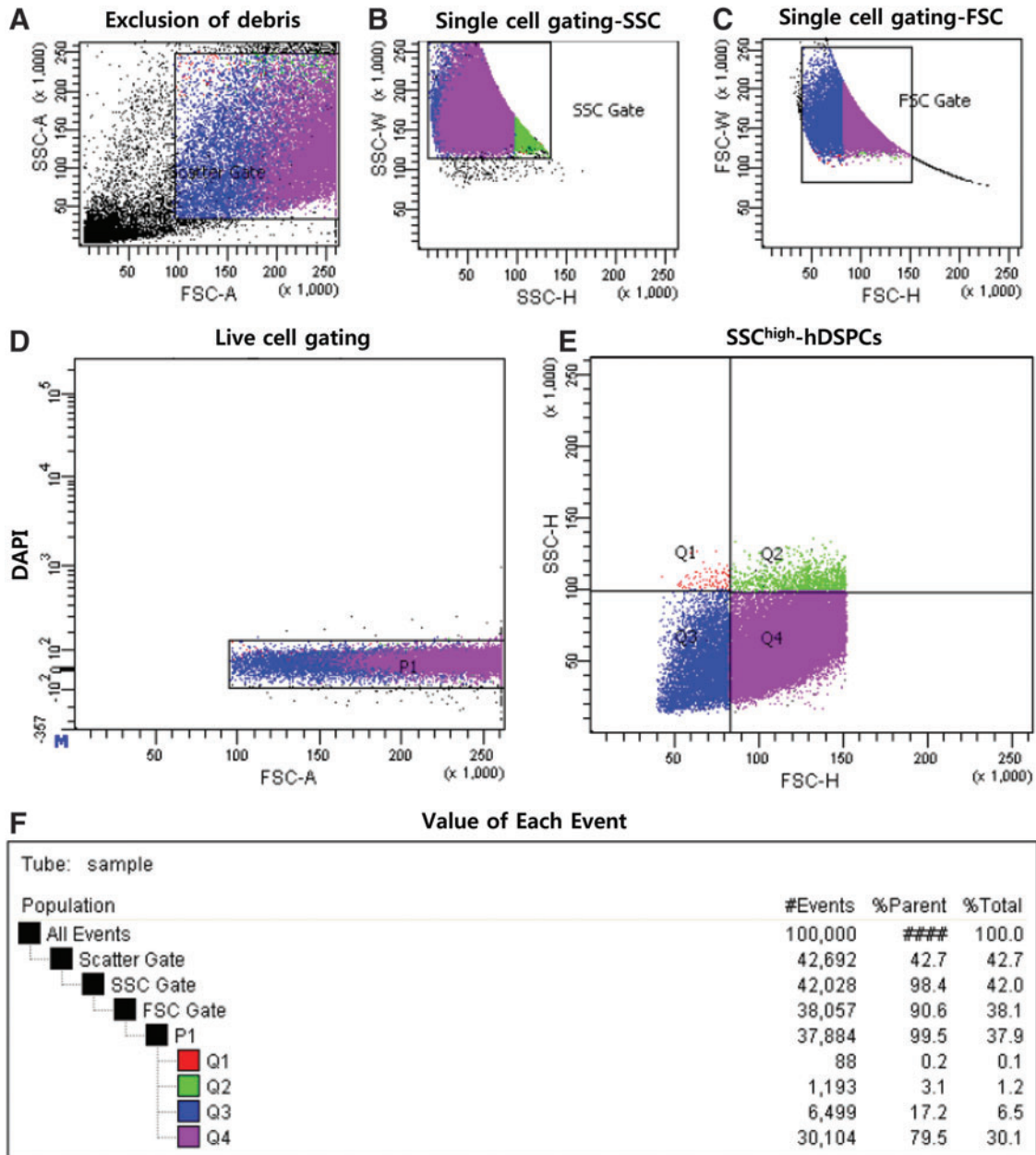


Supplementary Data

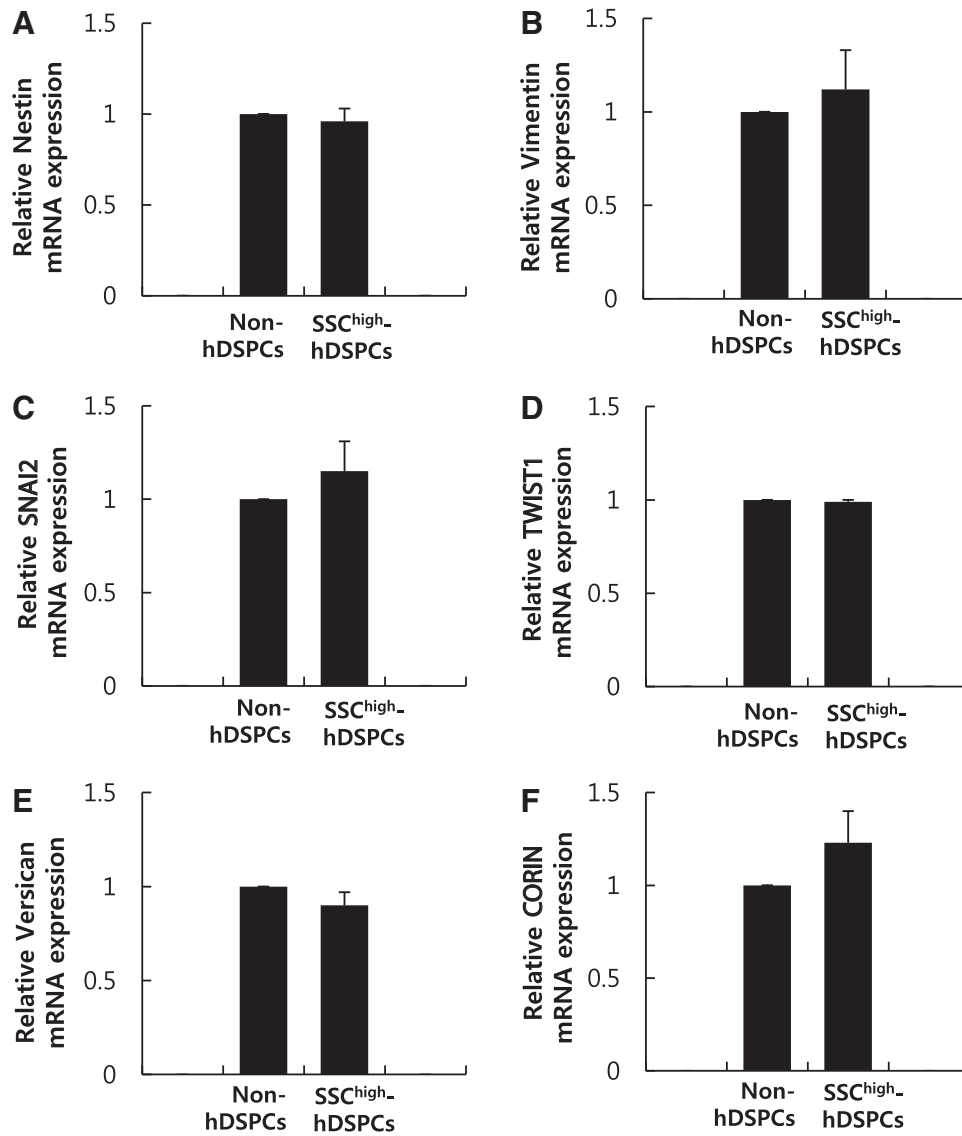
Supplementary Materials and Methods

For suspension culture of high side scatter (SSC^{high}) human dermal stem/progenitor cells (hDSPCs), the enriched SSC^{high}-hDSPCs were resuspended in the Dulbecco's modi-

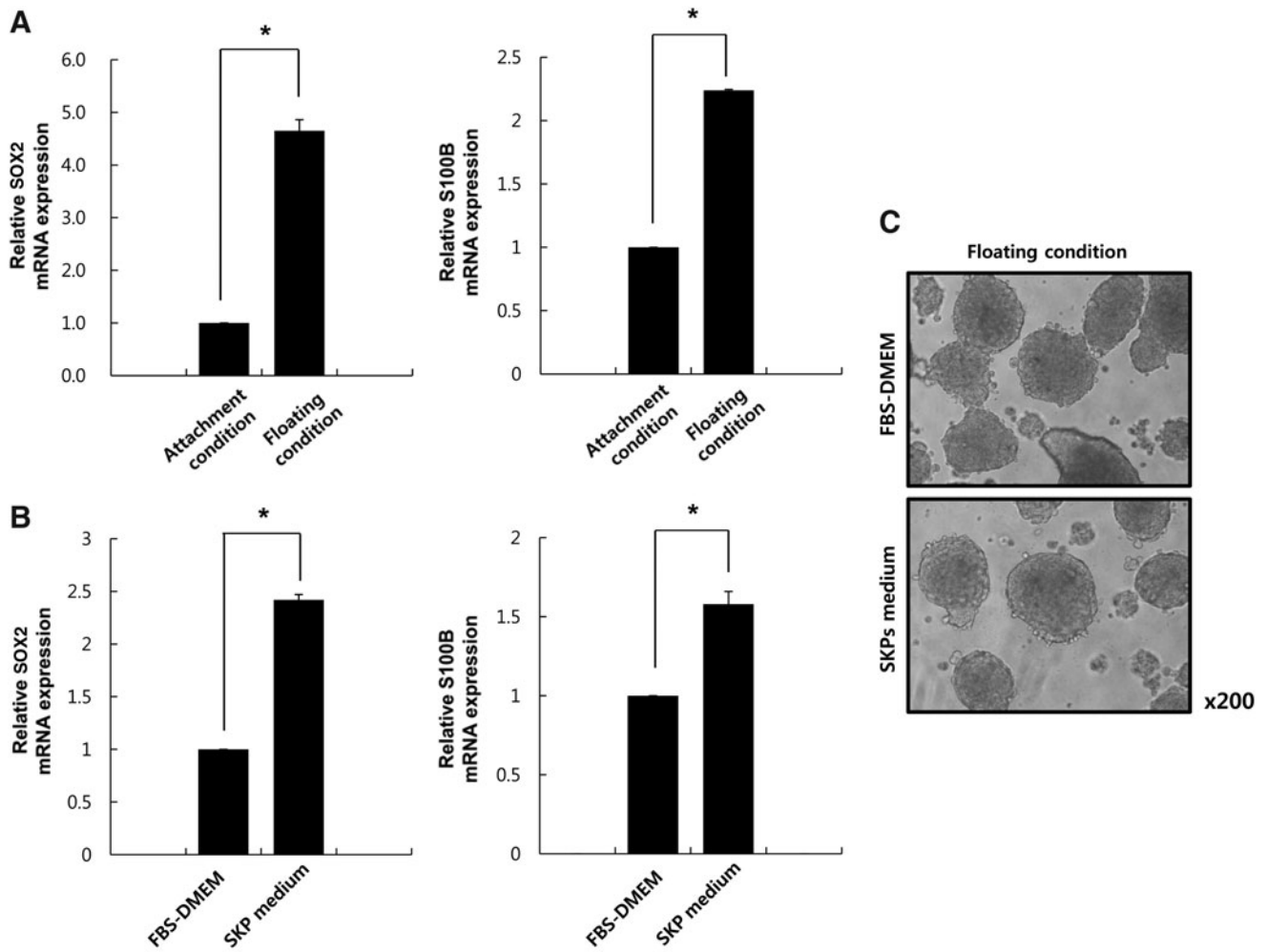
fied Eagle's medium/F12 (3:1; Invitrogen) containing 100 U/mL penicillin and 100 µg/mL streptomycin, 40 ng/mL FGF2, 20 ng/mL EGF (from R&D Systems), and B27 (Invitrogen) and then transferred to a HydroCell™ 3.5-cm Dish (Nunc). The cells were grown at 37°C in 5% CO₂ for 3 days.



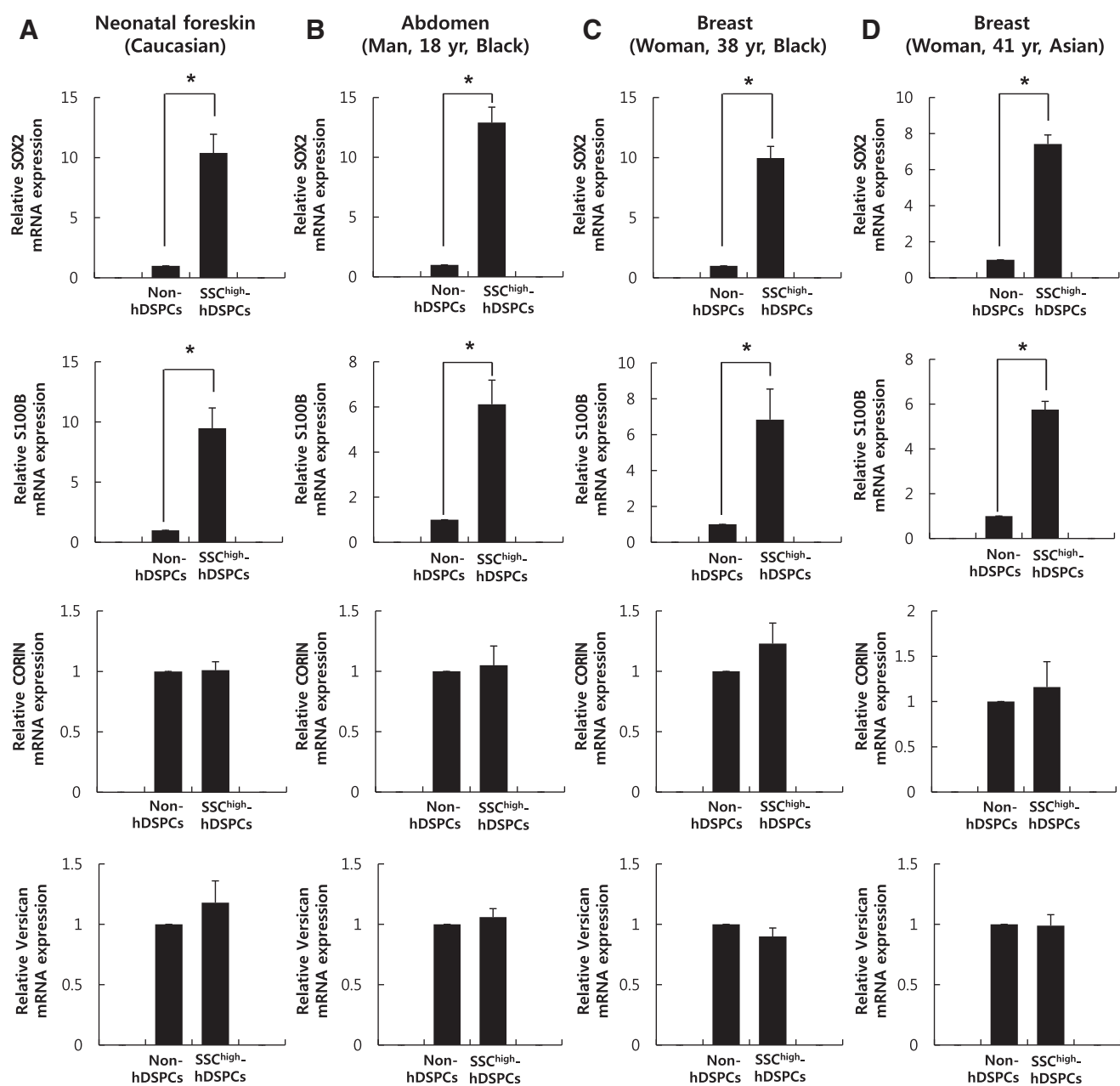
SUPPLEMENTARY FIG. S1. Purification of a SSC^{high}-hDSPC-enriched fraction. Cells were analyzed by flow cytometry as follows: (A) Cell debris was excluded at low and high extremes of FSC and SSC. (B, C) Doublets were excluded first by SSC and then by FSC-based time-of-flight analysis. (D) DAPI-positive (dead) cells were excluded. (E) Cells were divided into 4 groups (Q1: FSC^{low}SSC^{high}, Q2: FSC^{high}SSC^{high}, Q3: FSC^{low}SSC^{low}, and Q4: FSC^{high}SSC^{low}). (F) Both the cell number and percentage of each event versus percentage of total NHDFs are shown. A representative sample is shown ($n=3$). DSPCs, human dermal stem/progenitor cells; FSC, forward scatter; SSC, side scatter; NHDFs, normal human dermal fibroblasts; DAPI, 4',6-diamidino-2-phenylindole dihydrochloride.



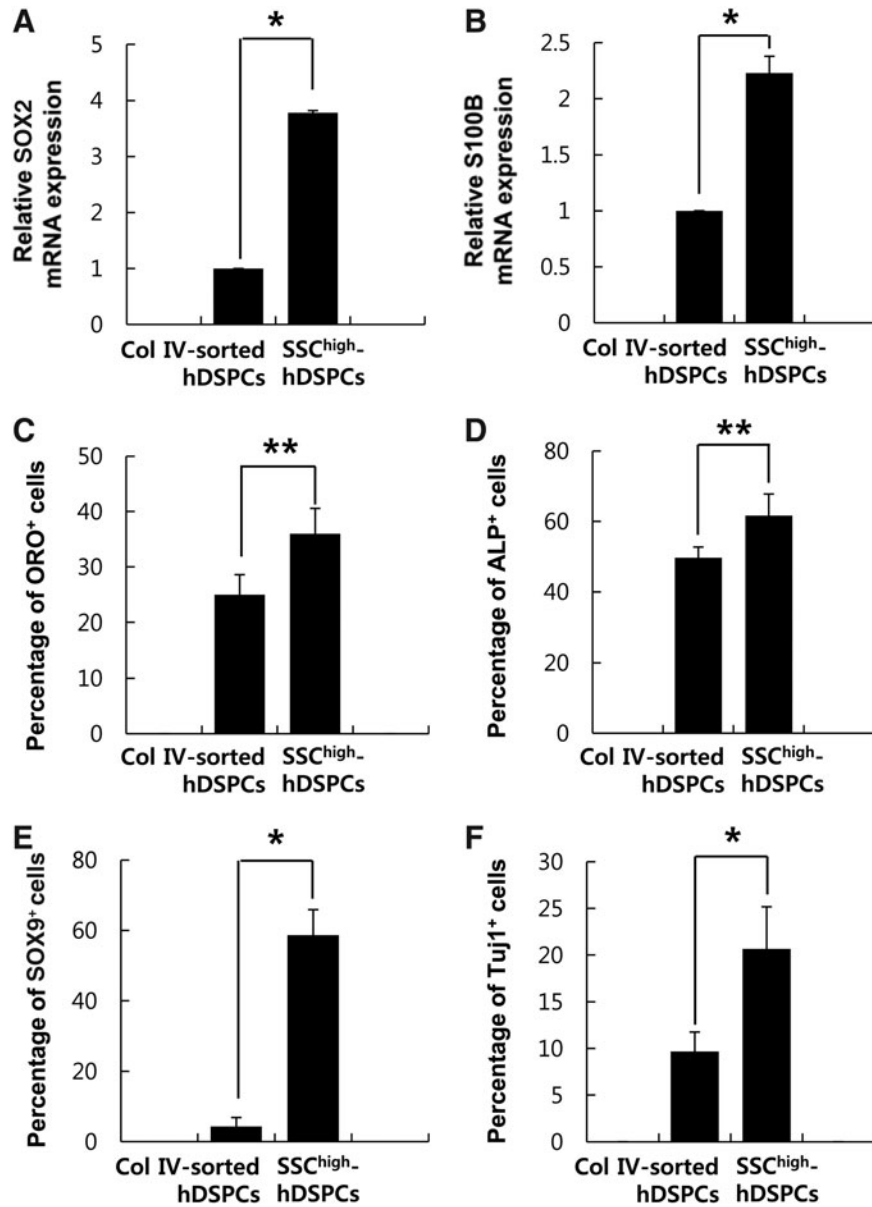
SUPPLEMENTARY FIG. S2. Characterization of SSC^{high}-hDSPCs. Real-time RT-PCR analysis of the SKP markers, (A) nestin, (B) vimentin, (C) *SNAI2* and (D) *TWIST1*, and the markers of dermal papillae, (E) versican and (F) *CORIN*. The data represent the mean±SD of triplicate runs. RT-PCR, reverse transcription-polymerase chain reaction; SKPs, skin-derived progenitors; SD, standard deviation.



SUPPLEMENTARY FIG. S3. Comparison of conditions for maintenance of SSC^{high}-hDSPC stemness. Real-time RT-PCR analysis revealed upregulation of *SOX2* and *S100B* mRNA expression. **(A)** SSC^{high}-hDSPCs were grown in 10% FBS-DMEM under an adherent and floating condition. **(B)** SSC^{high}-hDSPCs on a HydroCell™ plate was maintained under the 10% FBS-DMEM and SKP medium, respectively. **(C)** Phase-contrast microscope images of SSC^{high}-hDSPCs on the HydroCell™ plate were shown under the 10% FBS-DMEM (*upper panel*) and SKP medium (*lower panel*), respectively. The data represent the mean ± SD of triplicate runs. **P* < 0.01. FBS, fetal bovine serum; DMEM, Dulbecco's modified Eagle's medium.



SUPPLEMENTARY FIG. S4. Characterization of SSC^{high}-hDSPCs from different origins. Real-time RT-PCR analysis of SKP markers, *SOX2* and *S100B*, and markers of dermal papillae, *CORIN* and versican. **(A)** Neonatal foreskin (Caucasian), **(B)** abdomen (man, 18 years, Black), **(C)** breast (woman, 38 years, Black), and **(D)** breast (woman, 41 years, Asian). The data represent the mean \pm SD of independent experiments run in triplicate. * $P < 0.01$.



SUPPLEMENTARY FIG. S5. Comparison of collagen type IV-sorted hDSPCs and SSC^{high}-hDSPCs for stemness. (A, B) Real-time RT-PCR analysis of the SKP markers, *SOX2* and *S100B*. Histochemical or immunofluorescence staining analysis demonstrating the effectiveness of different conditions. (C) Oil-Red-O staining. (D) Alkaline phosphatase staining. (E) SOX9. (F) Tuj1. * $P < 0.01$, ** $P < 0.05$.